Cryostructuring of Polymer Systems. XXIX. Preparation and Characterization of Supermacroporous (Spongy) Agarose-Based Cryogels Used as Three-Dimensional Scaffolds for Culturing Insulin-Producing Cell Aggregates

Vladimir I. Lozinsky,[1] Lilija G. Damshkaln,[1] Konstantin O. Bloch,[2] Pnina Vardi,[2] Natalia V. Grinberg,[3] Tatiana V. Burova,[3] Valerij Y. Grinberg[1,3]

[1]A. N. Nesmeyanov Institute of Organoelement Compounds, Russian Academy of Sciences, Vavilov Street 28, 119991 Moscow, Russian Federation
[2]Diabetes and Obesity Research Laboratory, Felsenstein Medical Research Center, Sackler Faculty of Medicine, Tel-Aviv University, Petah Tikva, Israel
[3]N. M. Emanuel Institute of Biochemical Physics, Russian Academy of Sciences, Moscow, Russian Federation Address

ABSTRACT: Supermacroporous (spongy) agarose-based cryogels were prepared by a two-step freezing procedure (freezing at $-30°C$ followed by incubation at a warmer subzero temperature) and subsequent thawing. The cryogels were formed as cylinders in plastic syringes and as platelike samples in flat metal molds. The characteristic feature of the gel matrices thus obtained was their heterogeneous spongelike morphology with a system of interconnected gross (50–250-μm and larger) pores. The influence of the cryogenic processing regimes on the properties and porous morphology of such agarose cryogels was explored by flow-through analysis, optical microscopy, thermometry, and high-sensitivity differential scanning calorimetry. These biocompatible, spongelike matrices were used as three-dimensional scaffolds for culturing insulin-producing rat insulinoma cells self-assembled in multicellular spherical aggregates (pseudoislets). The cell morphology and functional activity of such pseudoislets indicate that supermacroporous agarose-based cryogels can be useful as a tool for engineering biohybrid insulin-producing tissue. © 2008 Wiley Periodicals, Inc. J Appl Polym Sci 108: 3046–3062, 2008

Key words: biopolymers; gelation; gels; hydrophilic polymers; polysaccharides

INTRODUCTION

Polymeric cryogels are gel matrices whose formation occurs in the course of the cryogenic treatment (moderate freezing/storing frozen/thawing) of initial solutions or colloidal sols of respective gel precursors.[1] One of the characteristic features of cryogels is their macroporosity, which is a system of large, interconnected pores. Such pores are created by the polycrystals of a frozen solvent, so they play

the role of porogens, and because each crystal grows until tight contact with a faucet of another crystal, this gives rise, after the system thaws, to the labyrinth-like porosity in the final cryogel.[1–3] Depending on the nature of the monomeric or polymeric gel precursors and their initial concentration and on the conditions of cryotropic gelation, one can prepare either macroporous cryogels (the pore size ranges from ca. 0.1 to 10 μm) or supermacroporous cryogels (also known as gigaporous cryogels) that have a spongelike morphology and pore sizes ranging from tens to hundreds of micrometers. The latter gel matrices have been shown to be promising materials as chromatographic media in the processes of separation of bioparticles such as cells or viruses[4–6] and as porous scaffolds for cell culturing.[7,8] In a previous work,[7] we demonstrated that supermacroporous, spongy agarose-based cryogels (ABCGs) were efficient scaffolds for the anchorage-dependent immobilization and further culturing of clonal insulinoma (INS-1E) cells capable of permanent insulin secretion. These scaffolds were cryogenically fabricated from

the agarose solutions, and this was followed by the grafting of reactive vinyl sulfone groups to the polysaccharide backbone with subsequent attachment of anchor gelatin molecules.

In turn, agarose, mainly an alternating copolymer of (1→3)-linked β-D-galactopyranose and (1→4)-linked 3,6-anhydro-α-L-galactopyranose,[9–11] is well known to be a constituent of agar–agar isolated from the red seaweed of the *Rhodophyceae* phylum.[12] Agarose is a noncharged neutral polysaccharide soluble in hot water, and resulting aqueous solutions are capable of fast gelling upon chilling below 50–30°C, depending on the molecular weight characteristics of the particular agarose specimen.[13–15] The physicochemical properties of such gels and fine mechanisms of agarose gelation in aqueous media have been thoroughly explored, and the crucial role of intramolecular and intermolecular hydrogen bonding in the thermoreversible formation of helix structures and junction knots of three-dimensional (3D) polymeric network has been established.[14,16–20] Because of their nontoxicity, biocompatibility, low nonspecific adsorptivity, and so forth, agarose hydrogels are widely implemented in biological practice, including activities dealing with the preparation and use of agarose-based gel supports, chromatographic resins, carriers, and scaffolds for the immobilization and cultivation of diverse animal cells (e.g., see refs. 21–27). In particular, wide porous scaffolds prepared by the directional freezing of preliminarily formed agarose hydrogels, their freeze-drying, and subsequent reswelling have been successfully employed as guides for the linear growth of axonal tissue,[23,25] and agarose cryogels, as mentioned previously, have been used as supermacroporous supports for the culturing of insulin-producing cells.[7] It was shown that such cryogel sponges prepared from agarose alone displayed very low adhesion properties for the anchorage-dependent growth of insulinoma INS-1E cells. Instead of the typical monolayer architecture, the cells formed clusters, morphologically resembling pancreatic islets. The formation of isletlike structures or pseudoislets is an inherent property of both pancreatic islet cells and insulinoma cells, resulting in homotypic β-cell communications required for insulin secretory responses.[28–30] These results suggest that close cell-to-cell contact improves the functional responsiveness of β-cells and that pseudoislets may be a useful research model in the study of β-cell function and prominent cell source for islet transplantation.

The aim of this work was to study the physicochemical properties and spongelike morphology of ABCGs and to evaluate the feasibility of these supermacroporous gel materials as 3D scaffolds for *in vitro* culturing of insulinoma cells self-assembled into 3D structures resembling native pancreatic islets.

EXPERIMENTAL

Materials

Type VII-A agarose (low gelling temperature), bovine serum albumin (BSA), and *C,N*-diphenyl-*N'*-4,5-dimethyl thiazol 2-yl tetrazolium bromide (MTT) were purchased from Sigma (St. Louis, MI). Cresyl Violet acetate dye was acquired from Aldrich (Milwaukee, WI). High-purity salts, alkalis, and acids used in chemical experiments were from Reakhim (Moscow, Russia). The Roswell Park Memorial Institute 1640 (RPMI 1640) culture medium, fetal calf serum (FCS), penicillin, streptomycin, and trypsin/ethylene diamine tetraacetic acid solution were all obtained from Biological Industries (Beit Haemek, Israel). The insulin radio immuno assay (RIA) kit was obtained from Sorin Biomedica (Saluggia, Italy). All aqueous solutions were prepared with deionized water.

Methods

Agarose cryogels were prepared in accordance with a patented procedure.[31] In brief, a specific amount of agarose powder was suspended in the volume of water required to reach the necessary final polymer concentration in the solution to be structured cryogenically. This suspension was then heated in a boiling water bath until the agarose dissolved. The sample was weighed before and after heating, and the amount of evaporated water was compensated; afterwards, the desired pH value was adjusted with a 1*N* solution of either HCl or NaOH. The hot (∼ 50°C) solution thus prepared was further used for the formation of ABCGs either in (1) cylindrical or (2) platelike-shaped samples. In case 1, 3 mL of the polymer solution was sucked into the plastic 5-mL syringe, sealed, and placed in the chamber of an FP 45 HP precision programmable cryostat (Julabo, Seelbach, Germany), in which the sample was frozen, kept at a desired minus temperature, and thawed at a rate controlled by the cryostat microprocessor (for particular regimes of cryogenic processing, see the Results and Discussion section). In case 2, a 2-mm layer of the polymer solution was poured into the stainless steel mold (0.5 × 9 × 12 cm^3), which was quickly installed in a flat pallet immersed in the coolant of the cryostat to freeze the system of interest. After completion of the process, the ABCGs thus prepared were exhaustively rinsed with deionized water up to neutral pH. For the cylindrical samples (case 1), this was done by the passage of the water through the syringes at a constant hydrostatic pressure equal to a 100-cm column of water. The ABCG plates were washed by immersion in the water bath with subsequent frequent changes of the liquid.

The water flow rates (mL/h) through the ABCG-containing syringes were determined under the

same conditions as those employed for rinsing such cylindrical cryogels. The experiments were carried out at 22 ± 1°C with five parallel samples; the obtained results were averaged.

When the dry matter content in the gel phase of spongelike ABCGs was determined, free water from the cylindrical samples that formed in plastic syringes under different freezing conditions was first removed by vacuum suction (water pump) for 5 min from each spongy cryogel through the bottom syringe outlet, and then residual capillary water was pressed out from ABCGs between layers of filter paper under a load of 100 g until the absence of a wet spot on the fresh filter. The weighed sample was then dried at 105°C up to a constant weight, and this revealed the value of the dry matter content.

Calorimetric measurements were carried out with agarose gel aqueous suspensions prepared as reported elsewhere.[32] The gel particle size in the suspensions was approximately 10 μm. The agarose concentration in the suspension was 3–5 mg/mL, as determined by the dry residue method. Calorimetric measurements were performed with a DASM-4 differential adiabatic scanning microcalorimeter (NPO Biopribor, Ruschino, Moscow Region, Russia) over a temperature range of 10–120°C and under excess pressure of 2.5 atm. The heating rate in all experiments was 1 K/min. Primary data processing was performed with WSCAL software (Institute of Protein Research, Pushchino, Russia). Excess heat capacity functions of the agarose double helix–coil transition were determined with NAIRTA software (Institute of Biochemical Physics, Moscow, Russia). The maximum temperature of the excess heat capacity function was considered the transition temperature (T_t). The transition enthalpy ($\Delta_t h$) was determined by the integration of the excess heat capacity function. The transition width ($\Delta_t T$) was determined as the ratio of $\Delta_t h$ to the height of the excess heat capacity peak.

Gel fusion temperatures were determined as follows. The syringes (with closed outlets) containing rinsed ABCG columns were used. Before the measurement, an approximately 5-mm-deep incision was made with a small scalpel on the top of each spongy cryogel, and a stainless steel ball 3.5 mm in diameter with a weight of 0.275 ± 0.005 g was placed in the incision. The upper part of the syringe was sealed with a rubber stopper, whereupon the syringe was placed into a water bath. The bath temperature was increased at the rate of 0.4 ± 0.1°C/min. The gel fusion point was determined as the temperature at which the ball fell down to the bottom of the syringe after passing through the fused ABCG.

The cryogels' morphology was studied with an Axiolab Pol optical microscope (Carl Zeiss Jena GmbH, Jena, Germany) equipped with a video-re-cording system (Sony, Tokyo, Japan). Thin (10 μm) sections of ABCGs were prepared with a Shandon Cryotome cryomicrotome (Thermo Electric Corp., Waltham, MA). Each section, placed on the microscope glass, was then covered with one drop of a 0.03% aqueous solution of Cresyl Violet acetate dye. After staining for 20 s, the excess dye was rinsed with water, and the superfluous water was removed with filter paper. Then, the section was poured with one drop of a fixing medium (a solution of 1 g of gelatin in 12 mL of 50% aqueous glycerol and 0.2 g of phenol as a bactereostatic agent) and sealed with a cover glass. Before the studies, the samples were stored at 4°C in a closed vessel.

Rat insulinoma (RINm) cells were cultured in a regular medium containing RPMI 1640 medium supplemented with 10% FCS, 10 mM 4-(2-hydroxyethyl)-1-piperazine ethanesulfonic acid, and 1% penicillin/streptomycin at 37°C in a CO_2 incubator (95% air/5% CO_2) as described elsewhere.[33]

The procedure of insulinoma cell seeding in cryogel sponges has already been described.[7] Briefly, the agarose cryogel disks (2 mm thick and 10 mm in diameter) were stored in 70% ethanol. Before use, the discs were carefully washed with sterile phosphate-buffered saline and regular medium. Thereafter, the medium was removed from the cryogel disk with gentle compression, and 0.2 × 10^6 RINm cells were injected into the disk placed in a plate of 24-well culture plates (Corning, Lowell, MA). Upon rapid swelling of a scaffold, the cells were imbibed by the spongy material. The samples were then cultivated in a CO_2 incubator at 37°C in 1 mL of regular medium per well. The medium was changed every other day. RINm cells, grown as a monolayer on the plastic surface of 24-well culture plates, were used as controls.

The morphology of cell clusters and cells' growth as a monolayer was observed under a Stemi 2000C binocular microscope (Zeiss) and a CK2 inverted microscope (Olympus, Tokyo, Japan). In some experiments, the cells were stained with 0.5 mg/mL MTT for a period of 3 h.

In the histochemical experiments, the samples of ABCGs containing cell clusters were embedded in paraffin wax. Thin sections (5 μm thick) were cut from each sample. After deparaffinization and dehydration, the sections were stained with hematoxylin–eosin (H&E) for routine examination.

Cell proliferation was determined by the MTT colorimetric assay, which reflects mitochondrial oxidative processes of living cells. Briefly, the cells were cultured in 24-well plates (2 × 10^5 cells/well), and then, after 24 and 96 h, the medium was replaced by the Krebs–Ringer bicarbonate buffer (KRBB) supplemented with 0.5 mg/mL MTT for a period of 3 h. The MTT-containing medium was then removed,

and the cells were exposed to 0.2 mL of dimethyl sulfoxide. The reduction of tetrazolium salt to formazan was quantified by the measurement of the optical density at 540 nm. Results were expressed as the percentage of MTT reduction.

The insulin secretion assay was carried out as follows. RINm cells were cultivated for 48 h within cryogel discs or on the plastic surface of 24-well plates. To estimate of K^+-dependent insulin secretion, RINm cells cultivated in spongy ABCGs or on a plastic surface for 2 days were preincubated for 1 h in glucose-free KRBB with 0.25% BSA and reincubated in the buffer at 37°C for an additional 2 h with 5 mM glucose and then with 5 mM glucose supplemented with 30 mM KCl. Supernatants were collected for the determination of insulin secretion. The stimulation index was calculated as the ratio of K^+-dependent insulin secretion to that of glucose alone. The level of insulin in the samples was estimated with an INSIK-5 radioimmunoassay kit (DiaSorin, Saluggia, Italy) that is 100% specific to rat insulin.

Analysis of variance was used to evaluate the statistical significance of differences between groups. The results are presented as mean values ± the standard deviation of independent, repeated experiments. P values less than 0.05 were considered significant.

RESULTS AND DISCUSSION

Prerequisites for the choice of experimental conditions feasible for the preparation of ABCGs

Conventional agarose hydrogels are well-known noncovalent (physical) thermoreversible gel matter, the gel-formation dynamics and properties of which depend on the molecular weight characteristics of the polymer, on the agarose concentration in the initial solution, and on the temperature of the system under gelling.[12–14,16,20] Indeed, aqueous solutions of agarose must be related to the fast-gelling systems because hot (60–50°C) 1–3% solutions of even specially developed, so-called low-gelling-temperature brands of this biopolymer, upon chilling to room temperature, lose their fluidity and are transformed into respective gels for several minutes. In this respect, such agarose solutions differ drastically, for instance, from concentrated aqueous solutions of atactic poly(vinyl alcohol) (PVA), the freezing–thawing of which results in the formation of PVA cryogels.[34,35] However, the initial PVA solutions are stable, at room temperature they do not gel for many days, and they transform into the mechanically weak hydrogels only upon very prolonged incubation.[36] Thus, such aqueous PVA solutions versus agarose-containing ones must be attributed to the slowly gelling systems.

Therefore, to prepare the ABCG, that is, the gel material, whose formation occurs exactly in the moderately frozen system (see the introduction), such conditions must be ensured that the initial polymer solution will take time to be frozen but will freeze before gelling to a considerable extent. This is to avoid the situation in which the gel formation will proceed either before the sample freezes or, at least, in parallel with freezing. In the former case, the already cured hydrogel will be cryogenically processed, and in fact, no pronounced gelation events will take place in the frozen specimen (such systems were comprehensively studied by Yokoyama et al.[37] about 20 years ago). In the latter case, there may be many elements at play, such as the polymer concentration, cooling rate, supercooling phenomena, and ratio of the gelling and freezing rates, that will influence the agarose cryotropic gel formation and will result in very poor reproducibility of the properties and porous morphology of the final ABCGs.

Thus, the crucial task to be solved to enable the successful formation of agarose cryogels was to decelerate the self-gelation of aqueous agarose solutions to an extent capable of providing the possibility of the system being frozen before gel formation.

Principally, there are two possible ways to achieve this goal:

1. By freezing an initially hot agarose solution very rapidly (e.g., in a liquid nitrogen bath).
2. By decreasing the self-gelation rate through the use of specific additives capable of partially inhibiting the sol-to-gel transition.

Experimental examination of the first option showed that this approach resulted in rather brittle macroporous gel materials, but their pore size was insufficient for the implementation of such cryogels as scaffolds for the culture of large animal cells inside the pore volume of the polymer carriers. The second approach enabled the preparation of ABCGs possessing the desired porosity when the solutes capable of partially interfering with the hydrogen-bond formation were introduced into the agarose solutions to be structured cryogenically.[31] These solutes are chaotropic agents (e.g., urea, guanidine hydrochloride, and LiCl), certain concentrations of which are able to decelerate somewhat the self-gelation of agarose solutions, thus allowing them to be frozen before the chilling-induced gelling of agarose and allowed the freezing-induced gelation process to be accomplished. However, high concentrations of urea or guanidine hydrochloride in such systems and their freezing at lower temperatures were required to obtain the necessary effect. A more convenient method was therefore the use of a pH shift toward the values capable of causing some ionization of

TABLE I
Influence of the pH Value on the Gelling Rate of the
Aqueous Agarose Solutions

Agarose concentration in the initial solution (g/dL)	pH value of the agarose solution at 50°C[a]	Time needed to reach a gel point at 20°C (min)[b]
2.5	~1	6.0
	4	4.5
	7	3.5
	8	5.5
	9.5	6.5
	10	10.0
	11	11.0
	12	12.5
	12.3	21.0
	12.6	30.0
	13	>40[c]

[a] Adjusted by the addition of a 1N solution of HCl or NaOH.
[b] ±0.5 min.
[c] Pronounced yellowing was observed.

agarose hydroxyl groups to create the same charges along the chains, thus giving rise to their certain repulsion. The latter, in turn, resulted in the elongation of the agarose self-gelation process (the data for the 2.5 g/dL solutions of agarose in water are exemplified in Table I).

Here, the protonation of agarose OH groups (e.g., at pH ~ 1) was found to be insufficiently effective because the time needed to reach the gel point increased from about 3.5 (pH 7) to only 6 min, whereas the deprotonation of agarose hydroxyls (obviously, primary ones in general) gave rise to a marked increase in the gelation time, especially at pH values higher than ~ 12. However, when preparing hot agarose solutions with relatively high alkali contents (e.g., at pH ~ 13), we observed expressed yellowing of the system. Such an effect testified to the oxidative degradation of agarose macromolecules under the conditions employed. Thus, in subsequent studies on the preparation of ABCGs, we adjusted the pH values of the initial agarose solutions to approximately 12.6. In addition, preliminary experiments revealed that with respect to their macroporosity and physicomechanical qualities, the agarose cryogels most suitable for the creation of cell culture scaffolds originated from the 2.5–3.0 g/dL solutions of the used brand of agarose (see the Materials section), so these polymer concentrations were then implemented in subsequent research.

Influence of the conditions of cryotropic gel formation on the features of the porous morphology of ABCGs

As a rule, in the processes of cryotropic gel formation, the freezing conditions are of great significance

for both the physicochemical properties and porous morphology of the resulting cryogels.[1] Therefore, in this work, we explored the influence of freezing regimes on the texture of spongelike ABCGs.

It was first established that supermacroporous agarose cryogels could be successfully prepared only if the freezing temperature did not exceed −25 to −30°C when we were dealing with the 2.5–3 g/dL solutions of the polymer (pH ~ 12.6 and temperature ≈ 50°C). Under warmer freezing conditions in the coolant bath, the crystallization rate was insufficient to devoid the agarose self-gelation phenomena. Consequently, freezing was performed at −30°C both when the platelike samples were being formed and for the agarose solutions poured into plastic syringes. The duration of this step was always 1 h, whereupon the frozen specimens were incubated (stored frozen) for 23 h at −30, −20, −10, or −5°C and then defrosted at the rate of 0.3°C/min. Thereafter, we measured the flow rates of water through respective ABCG columns (see the Methods section) to evaluate the influence of the frozen storage temperature on the hydrodynamic characteristics of cylindrical cryogel samples. Such flow-through rates, as earlier shown for spongelike polyacrylamide cryogels,[38] are sensitive indicators of macropores' sizes. In all similar cases, the lower the freezing temperature was, the smaller the size was of porogen particles (polycrystals of frozen solvent), and hence the smaller the size was of macropores in respective spongy cryogels. In turn, the smaller the pore cross section was, the lower the flow rate was through similar columns at equal hydrostatic pressure because the flow resistance increased. The experimental results obtained for ABCG columns are summarized in Table II.

It was found that cryogels based on 2.5 and 3.0 g/dL solutions of agarose and formed in equal temperature regimes were similar with respect to their flow-through characteristics, whereas the temperature of the second step of the cryogenic treatment, that is, frozen storage, had a presumable effect on the hydrodynamic characteristics of such gel matrices; that is, the lower the temperature was, the lower the flow rate was. On the one hand, these data meant that such a narrow range of polymer concentrations did not have a significant influence on the macroporous morphology of ABCGs. On the other hand, the dependence of the flow-through rates on the frozen storage temperature meant that the cryostructuring processes did not stop after the specimen froze at −30°C and further continued upon the incubation of the said frozen samples at warmer subzero temperatures, despite the fast gelling abilities of agarose. This latter conclusion is in good agreement with the known concepts of cryotropic gel formation,[1–3] which proceeds in the so-called unfrozen liq-

TABLE II
Hydrodynamic Characteristics of the ABCG Columns

Agarose concentration in the solution before cryostructuring (g/dL)[a]	Temperature of the stage (°C)		Flow rate of water through the 3-mL ABCG columns (mL/h)[d]
	Freezing[b]	Storing frozen[c]	
2.5	−30	−5	233 ± 6
		−10	215 ± 2
		−20	210 ± 9
		−30	201 ± 2
3.0	−30	−5	233 ± 4
		−10	217 ± 5
		−20	213 ± 4
		−30	209 ± 1

[a] pH = 12.6.
[b] One hour.
[c] Twenty-three hours.
[d] At a hydrostatic pressure of 100 cm of the water column.

uid microphase (ULMP),[1,39] in which soluble gel precursors are concentrated, thus promoting the gelation processes. In the absence of structuring phenomena after freezing of the system is completed, the influence of the temperature of the second step of the cryogenic treatment on a gel-morphology-sensitive parameter such as the flow rate of water through the ABCG columns is of no concern: a quick freeze forms the wide pores, and further changes in their architecture are not possible because of the loss of necessary mobility of the system's components. Indeed, the differences in the flow rate values for the samples stored frozen at −30 and −5°C (end points over the studied range) were not very large, approximately 10–15%, but the differences were reliable and surely exceeded the experimental errors.

At the same time, the fact that flow rate values for the ABCG columns incubated frozen at a higher temperature were larger than those of cryogels formed at a lower temperature (Table II) suggested the occurrence of ice recrystallization phenomena in systems frozen at −30°C and then incubated at −20, −10, or −5°C. This should result in the enlargement of ice polycrystals and, consequently, in the widening of pore sections in the defrosted spongelike ABCGs. However, not only did the ice change during such an incubation, but so did the ULMP (particularly its volume), the concentration of dissolved components, the morphology of the polymer network formed, and so forth. No doubt, these processes result in differences in the properties of the proper gel phase (walls of macropores) of spongy ABCGs prepared under various frozen storage conditions. Some differences were observed in the thermophysical characteristics, such as the fusion temperatures, of these cryogels (as discussed later). In addition, overall textural features of respective ABCGs were revealed with optical microscopy of thin sections of these gel materials.

For instance, micrographs in Figure 1 present the morphology of ABCGs formed on the basis of 3 g/dL solutions of agarose under the same thermal conditions used for cylindrical cryogels, the hydrodynamic properties of which are summarized in Table II. The photographs of the left column in Figure 1 are typical of the cross sections close to the centers of ABCG cylinders (the sections were made at about the half of the samples' height), and the right column photographs show the longitudinal sections.

Such ABCGs prepared from agarose solutions poured into plastic syringes and frozen by immersion in a liquid coolant (ethanol) in a cryostat chamber (see the Methods section) possessed anisotropic macroporosity; that is, the morphology of cryogels seen with an optical microscope was rather dissimilar in width and height to the cylindrical specimens. Cross sections of the samples resembled a cobweb with mesh sizes of approximately 50–250 μm [Fig. 1(a)–(d)]. Longitudinal sections [Fig. 1(e)–(h)] contained mainly the oriented lamellar elements, being the sections of thin gel walls of macropores. In general, the anisotropic texture of all these cryogels meant that the growth of ice crystals upon the samples' freezing in this case occurred mainly along the axis of a cylinder. In turn, one can surmise that similarly directed ice crystallization was a result of the specific shape of syringes: the agarose solution in the small volume of the outlet nozzle was chilled and frozen earlier than the major part of the solution in the syringe. This quickly frozen small volume could perform as a primary germ for further ice formation, essentially from the bottom toward the top of cylindrical specimens. It is noteworthy that the morphology of ABCGs, particularly in the micrographs of longitudinal sections in Figure 1(e)–(h), were very similar to those reported recently by Van Vlierberghe et al.[40] for cryogenically structured supermacroporous gels prepared by freeze drying of cross-
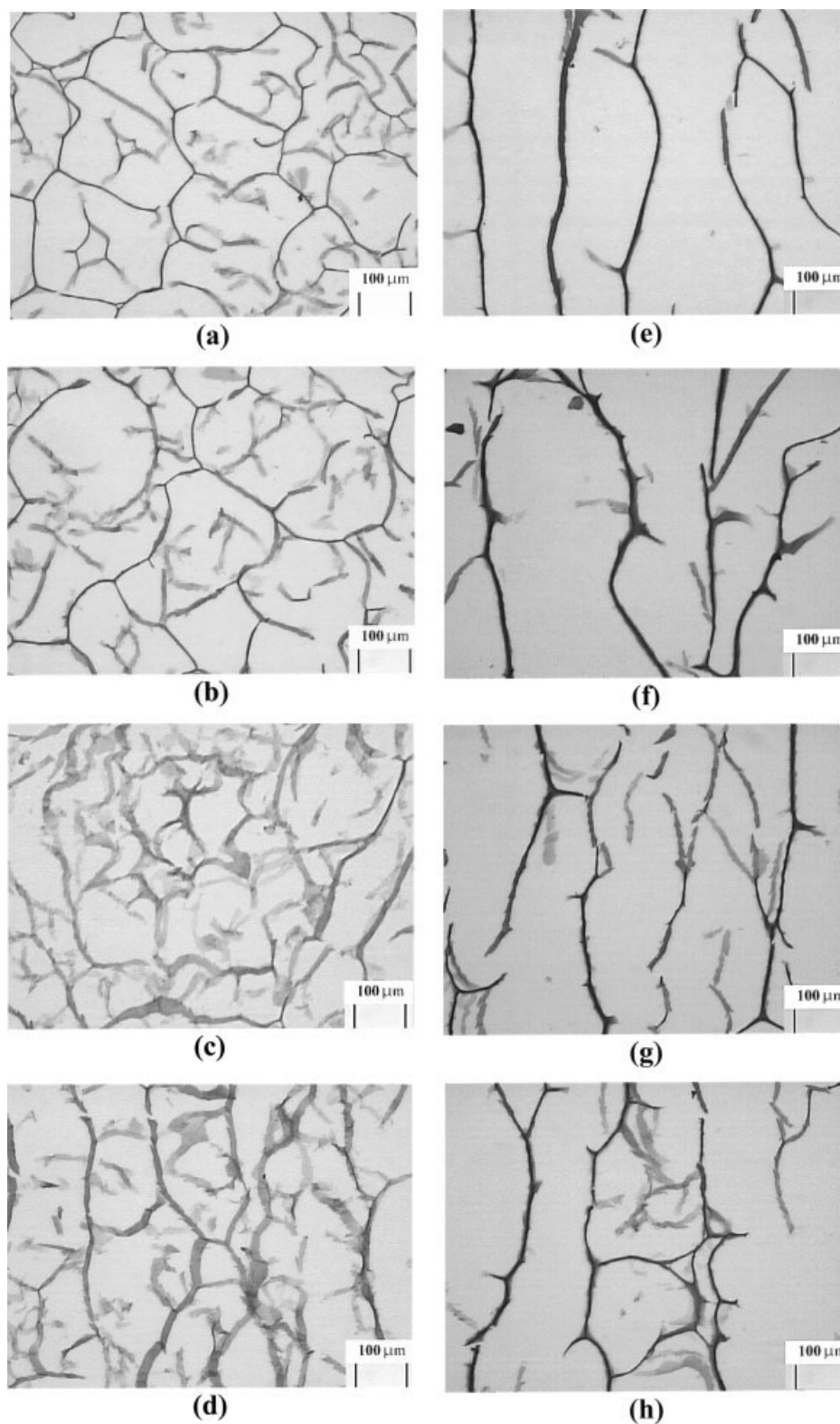
Figure 1 Optical microscopy images of 10-μm (thin) sections of cylindrical ABCGs that we prepared by freezing 3 g/dL aqueous agarose solutions (pH ≈ 12.6) at −30°C for 1 h, then incubating them frozen for 23 h at (a,e) −5, (b,f) −10, (c,g) −20, or (d,h) −30°C, and finally thawing them at a rate of 0.3°C/min. (a–d) Cross sections and (e–h) longitudinal sections were stained with Cresyl Violet.

linked gelatin hydrogels. This similarity supports the notion of the universality of mechanisms governing the formation of such spongy gel matrices with interconnected gross pores.

As for the peculiarities of the pore structure and pore size of the cryogel samples formed under different frozen incubation conditions, we observed a rather irregular heterogeneous morphology for all these samples (Fig. 1) and a somewhat denser network with smaller meshes in the cross sections of samples incubated frozen at lower temperatures (−30 and −20°C) in comparison with the ABCGs stored frozen at higher temperatures of −10 and especially −5°C [cf. micrographs in Figs. 1(d) and 1(c) with Figs. 1(b) and 1(f), respectively]. In addition, a more irregular pattern was inherent in the longitudinal sections of agarose cryogels kept frozen at lower incubation temperatures [cf. micrographs in Fig. 1 in the order of 1(e), 1(f), 1(g), and 1(h)]. Such differences in the pore structure of ABCGs prepared under various freezing conditions were the obvious reason for the observed variations in the flow-through characteristics of respective ABCG columns (Table II). From our viewpoint, all these data testify that a primary irregular macroporous gel system is quickly formed at a temperature of −30°C, and subsequent slower changes in the porous morphology of the specimens are induced only upon the prolonged incubation of frozen samples at warmer subzero temperatures: the higher the temperature of the still macroscopically frozen system is, the more pronounced the changes are.

The morphology of the gel phase (the walls of macropores) in spongy ABCGs was observed microscopically at a resolution 5 times that of Figure 1. Micrographs in Figure 2 demonstrate the fragments of gel matter in the same heterophase agarose cryogels depicted in Figure 1. The surfaces of the macropores are not smooth and even have in many areas an indented relief resembling dandelion leaves [e.g., Fig. 2(f,h)]. Apparently, such morphology of the gel phase arose because of the physicomechanical influence of stresses (accompanying ice crystallization and recrystallization) on the brittle, highly concentrated agarose hydrogel within the space of these walls, thus resulting in the formation of small cracks.

In turn, the general pattern inherent in the cross sections of cylindrical ABCG can be viewed by a microscope magnification 2 times smaller that in Figure 1, which reveals structural heterogeneity from the periphery to the center (it is because of such pronounced heterogeneity that we did not subject the microscopy images to available procedures of mathematical treatment for obtaining quantitative data on porosity characteristics; the standard deviations of the resulting values were too great).

The micrographs in Figure 3 show the typical morphology of three different areas: peripheral, intermediate, and central parts of cryogel samples frozen at −30°C and further incubated also at −30 [Figs. 3(a–c)] or −5°C [Figs. 3(d–f); ABCG samples incubated at −20 and −10°C had less pronounced differences and, therefore, are not shown in Fig. 3]. The pictures demonstrate that gross lengthy pores (200–400 μm in diameter) were formed inside the syringe just near its wall [Fig. 3(a,d)], where the heat sinking upon freezing of the agarose solution was the most intensive. Closer to the sample's center, the observed pattern changed across the mixed (with respect to the texture) intermediate areas [Fig. 3(b,e)] to the cobweb structures [Fig. 3(c,f)], demonstrating pores of a different shape and a smaller diameter. The morphology of these three regions of cross sections (Fig. 3) was more heterogeneous in the case of ABCG prepared by freezing and incubation at −30°C [Fig. 3(a–c)] compared to that of the cryogel frozen at −30°C and then stored frozen at −5°C [Fig. 3(d–f)]. This observation was noted particularly in the peripheral and intermediate zones of the cross sections. Indeed, such differences in the morphology of samples incubated frozen at different subzero temperatures also indicate that the transformation of the cryogel texture took place exactly in the moderately frozen system at temperatures warmer than −30°C. In other words, somewhat more favorable heat-transfer conditions near the syringe wall facilitated the growth of ice crystals from the periphery to the center. At that, some portion of agarose matter was displaced from the periphery toward the central axis of the cylinder, resulting in the formation of a denser network (a rather similar picture was also observed[37] upon directional freezing of the preset agarose hydrogels). At the same time, subsequent incubation of samples frozen inside the syringes at warmer subzero temperatures (over the studied range of −20 to −5°C) caused, despite the apparent solid state of the specimens, significant changes in the morphology of respective ABCGs, lowering their macroheterogeneity. The reason for such changes could possibly be ice recrystallization processes, the intensity of which generally increase with a rise in temperature.

Because ABCGs were to be used as scaffolds for cell cultures, we also studied structural peculiarities of the 2-mm-thick platelike cryogels prepared under the optimum conditions of cryostructuring, that is, freezing at −30°C with subsequent incubation (frozen) at −5°C. Micrographs in Figure 4 (with the same microscope magnification used in Fig. 3) present the texture of such ABCGs sectioned: parallel with the flat surfaces of the sample, that is, athwart to the main direction of ice crystals growth [Fig. 4(a)], and along with that, namely, from the mold bottom upward [Fig. 4(b–d)]. In the latter case, three
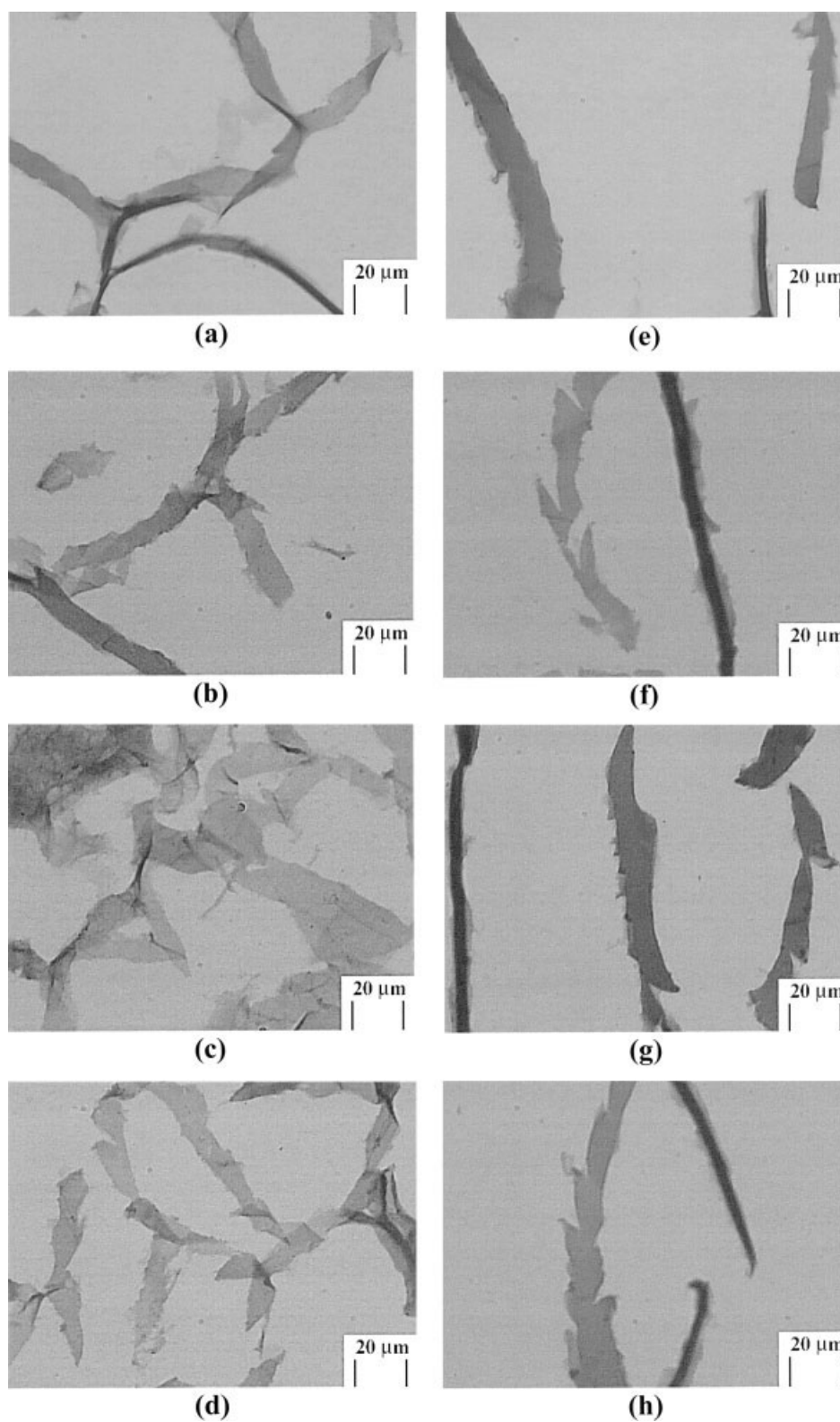
Figure 2 Micrographs of the same samples shown in Figure 1 (thin ABCG sections) visualized at a 5 × higher microscope magnification.

regions were examined: in the vicinity of the bottom surface of the platelike sample [Fig. 4(b)], around half of the sample's height [Fig. 4(c)], and in the vicinity of the top surface [Fig. 4(d)], that is, in the order reflecting the direction of porogen (ice crystals) propagation.
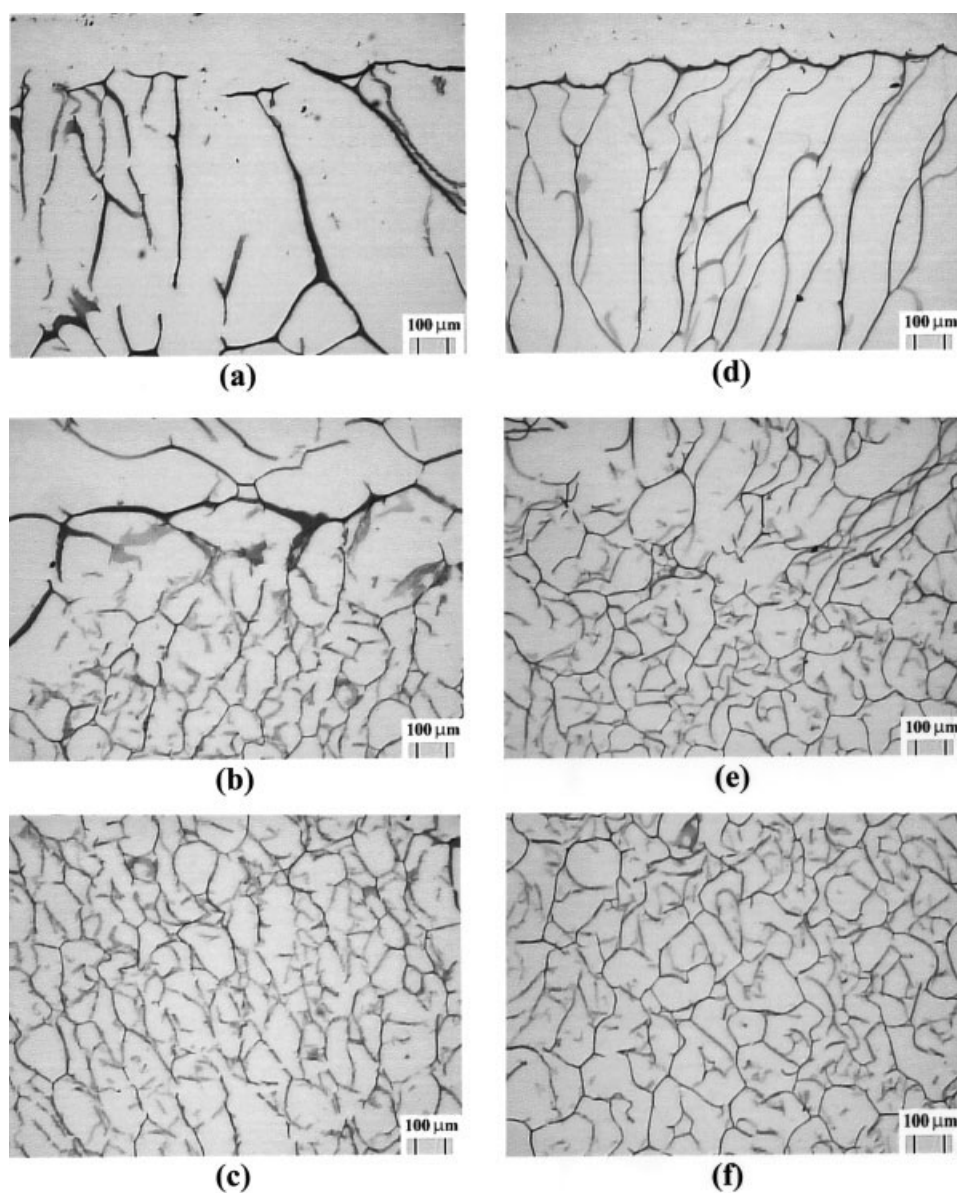
Figure 3 Optical microscopy images of different regions of the cross sections of cylindrical ABCGs that, upon cryostructuring, were incubated frozen at either (a–c) −30 or (d–f) −5°C: (a,d) peripheral regions, (b,e) intermediate zone, and (c,f) central part. The microscope magnification was 2 × less than that in Figure 1.

The cellular morphology of this spongy gel material can be clearly seen in the cross section [Fig. 4(a)], in which the pore size is markedly larger than that in the cylindrical ABCG prepared under the same freezing conditions [Fig. 3(d–f)]. Such differences in pore diameters were probably the result of distinct heat-transfer conditions in the course of the freeze processing of an agarose solution either inside the plastic syringe or poured in a thin layer onto the flat stainless steel mold. This fact once again testifies to the high sensitivity of agarose cryotropic gelation to the freezing regimes. It is of interest that a honeycomb-like shape of the mesh in Figure 4(a) turned out to be similar to that in agarose scaffolds fabri-cated by Stokols and Tuszynski[23,25] using the uniaxial freezing of a 3% agarose hydrogel and its subsequent freeze-drying. Such a similarity obviously indicates that in both the preformed agarose hydrogel and an alkaline agarose solution, the solvent (water) is transformed into a close crystalline form upon freezing.

Moreover, the general character of structural variations in the platelike samples from bottom to top turned out to be very similar to the pattern observed by Yakoyama et al.[37] for directionally frozen preset agarose hydrogels. In the case of ABCGs, the micrograph in Figure 4(b) shows the open-pore character (with wide inlets 300–400 μm in diameter) of the top
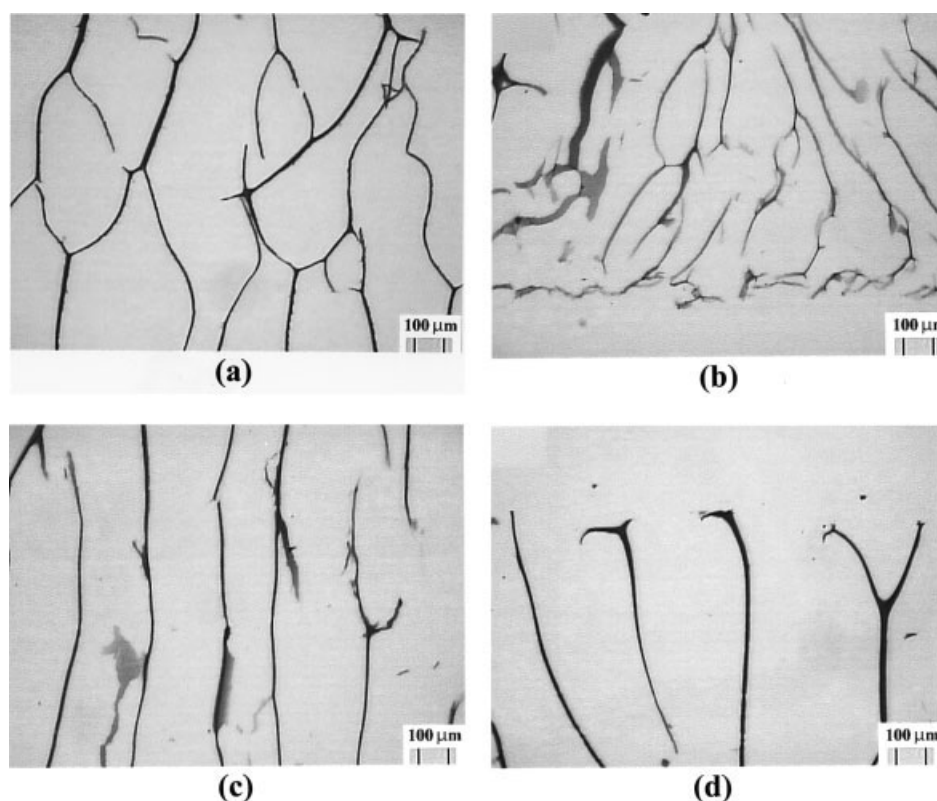
Figure 4 Optical microscopy images of thin sections of platelike ABCGs that we prepared by freezing 3 g/dL aqueous agarose solutions at −30°C and further incubating them frozen at −5°C: (a) cross section around half of the sample's height and longitudinal sections of respective areas (b) near the bottom surface, (c) in the middle region, and (d) in the vicinity of the top surface of the approximately 2-mm-thick platelike agarose cryogel.

surface of such platelike matrices as a compulsory requirement for the efficient, unhindered seeding of 3D scaffolds with the cells to be cultured.[26,27] The macropores in the middle part of the platelike agarose cryogel are virtually straight capillaries of 200–300 μm in cross section [Fig. 4(c)], whereas near the bottom surface of such ABCGs, a certain decrease in their size is observed [Fig. 4(d)]. In this area, the gel morphology resembles the intermediate zone in cylindrical cryogels [Fig. 3(b,e)]. However, the formation of such dense cobweblike morphological elements in the platelike ABCGs as in the central regions of cylindrical samples [Fig. 3(c,f)] was not traced. Hence, the comparison of the textures of ABCG cylinders and plates revealed marked differences. We attribute this result, on the one hand, to the small layer (∼ 2 mm) of agarose solutions to be frozen and to the better heat sink through the metal matter of a flat mold than through the plastic wall of a syringe. Therefore, the freeze-induced structuring in a flat, thin layer had time to leave behind substantial displacement of agarose from the bottom to the top of a platelike sample and the formation of dense networks similar to those adjacent to the axis of cylindrical ABCGs. That is why, when further preparing ABCG scaffolds for cell culture, we froze the samples that were thus no thicker than 2–3 mm.

Cryoconcentrating effects

Micrographs in Figures 1–4 clearly show that the proper gel phase in supermacroporous spongy ABCGs occupies a reduced portion of the material's bulk, whereas a larger portion is taken by the space of the pores. Hence, all the agarose matter, which was dissolved in the initial solution and then was uniformly distributed over the volume of the ordinary agarose hydrogel formed upon the simple chilling of such a solution (i.e., without its freezing–thawing), in the case of the cryogel-type material, was concentrated within the thin walls of macropores as a result of cryoconcentrating effects. These effects (increasing the solute concentration in ULMP as the major amount of the solvent is crystallized off) are characteristic of cryotropic gelation processes in general.[1] To evaluate the extent of such an effect on ABCGs, we removed free (capillary) water from the spongy material and measured the dry matter content in the gel phase of these cryogels (see the Methods section). The values found are summarized

TABLE III
Agarose Concentration in the Walls of the Macropores in the ABCGs

Agarose concentration in the solution before cryostructuring (g/dL)[a]	Temperature of the stage (°C)		Dry matter content in the gel phase of the spongelike ABCGs (%)
	Freezing[b]	Storing frozen[c]	
2.5	−30	−5	24.5 ± 1.1
		−10	24.2 ± 0.6
		−20	23.9 ± 0.7
		−30	23.3 ± 0.5
3.0	−30	−5	25.1 ± 1.8
		−10	24.3 ± 1.6
		−20	24.1 ± 1.0
		−30	23.9 ± 1.6

[a] pH = 12.6.
[b] One hour.
[c] Twenty-three hours.

in Table III, from which the following observations were made.

At first, the average polymer concentrations in the pore walls of supermacroporous ABCGs formed from the 2.5–3.0 g/dL solutions of agarose under various thermal conditions turned out to be rather close to each other, namely, of the order of 23–25%. Such a similarity once more testifies to the rather slight differences in the properties of agarose cryogels being dependent on the polymer concentration over the indicated initial narrow range. On the other hand, the values of Table III show that the agarose concentration in the gel phase of heterophase ABCGs increased significantly compared with that of feed solutions, to the extent of an order of magnitude. Second, although the differences in the values of the dry matter content for the samples stored frozen at various subzero temperatures during the preparation process were not too large, the main trend was noticeable: the lower the frozen incubation temperature was, the lower the polymer concentration was in the pore walls of the respective spongelike ABCG. Obviously, a higher dry matter content in the pore walls of agarose cryogels incubated frozen at −5°C (Table III) and the increased values of their fusion temperature (see the next section) compared to those of the samples kept frozen at lower minus temperatures were the results of the already mentioned additional structuring processes. The latter could occur to a greater extent during the storage of samples frozen just at −5°C rather than at −10, −20, and, moreover, −30°C because of the higher thermal mobility of solutes in ULMP and lower medium viscosity.

The increase in the polymer concentration in the gel phase of supermacroporous agarose cryogels (Table III) compared to the solution of gel precursors is the typical effect of cryotropic gelation.[1] For instance, when polyacrylamide cryogels were formed from the monomeric precursors, namely, on the basis of a

3% solution (in water or formamide) of a mixture of acrylamide and N,N′-methylene-bisacrylamide, the dry matter content in the pore walls of the resulting spongy gel materials reached 20–30%, depending on the initial comonomer ratio and cryopolymerization temperature.[41] In the case of macromolecular precursor and cryotropic gel formation via the chemical crosslinking of the polymer in a moderately frozen system, such as polystyrene crosslinking with p-xylylene dichloride in a frozen nitrobenzene medium,[42] the polymer concentration arose from about 1–4% in the feed to ∼ 25–33% in the gel phase of spongy polystyrene cryogels. Hence, the polymer concentration in the pore walls of noncovalent agarose cryogels that we studied was of the same order as that in the pore walls of covalent (chemically linked) cryogels formed from similar (with respect to the gel precursor concentration) initial solutions.

The cryoconcentrating effects impart enhanced mechanical strength to the walls of macropores in polymeric cryogels. Thus, capillary water from the spongelike ABCGs fabricated according to the procedure described here can be squeezed off with moderate compression of the cryogel sample without destroying the heterophase gel material, whereas common agarose hydrogels are well known to be very fragile and are easily fragmented even when pressed by the fingers of a human hand.

A considerable increase in the polymer concentration from only 2.5–3% in the initial agarose solutions to about 23–25% in the gel phase of spongy ABCGs as a result of cryotropic gel formation makes this process different from that used for the preparation of so-called superporous agarose gels.[43–45] The latter are formed by the chilling-induced (but without freezing) gelation of a rather viscous (polymer concentration ≈ 6%) and hot agarose aqueous solution in the composition of a liquid two-phase emulsion consisting of, apart from the aqueous phase, heptane

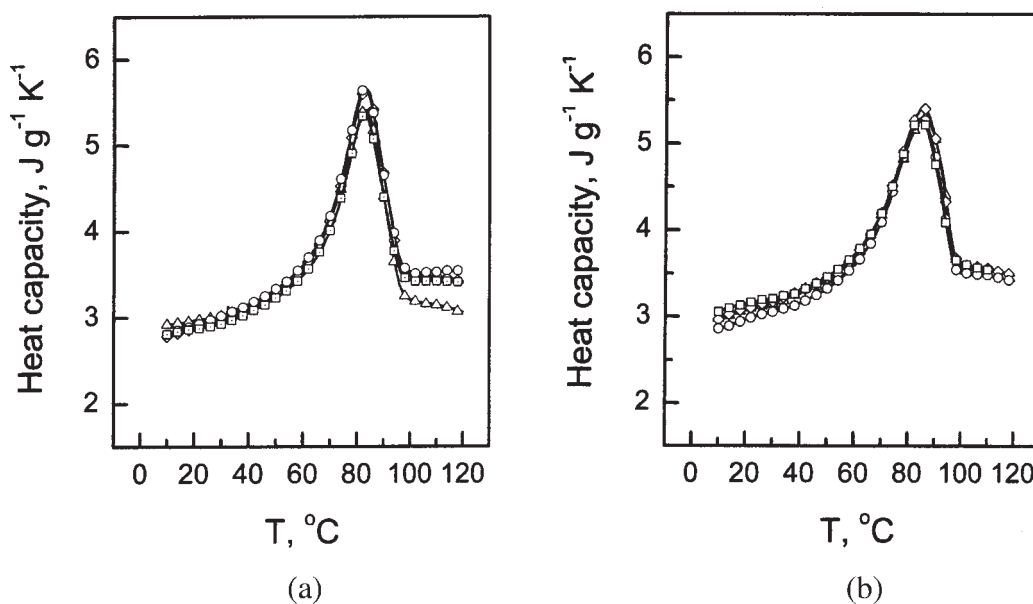**Figure 5** Thermograms of the agarose cryogels and gels: (a) cryogels formed at frozen storage temperatures of (△) −5, (◇) −20, and (○) −30°C with polysaccharide concentrations in the precursor solution of (△,◇,○) 2.5 and (□) 3.0 g/dL and (b) ordinary agarose gels obtained upon the cooling of the polysaccharide precursor solution at concentrations of (△) 1.25, (◇) 2.5, (○) 3.75, and (□) 5.0 g/dL.

or a cyclohexane solution of Tween 80. At definite ratios of aqueous and water-immiscible organic phases, an interpenetrating, continuous, liquid two-phase system can be prepared with intense stirring, and subsequent chilling of this liquid emulsion below the agarose set temperature gives rise to the formation of heterophase gelled matter. The organo-soluble components are then extracted through the system of interconnected large pores through rinsing with aqueous ethanol and then water. In such a case, the agarose concentration in the gel phase of the resulting macroporous material remains the same as that in the aqueous phase of the initial emulsion before its gelling. Therefore, the pronounced fragility inherent in the common homo-phase 6% hydrogel of agarose is conserved in the pore walls of such superporous agarose gels that have a spongelike morphology. However, these sponges, especially the plates of small thickness, are rather brittle.

In turn, the spongy morphology of ABCGs allows the removal of the capillary-bound liquid with gentle compression. Then, after the placement of the thus pressed-off agarose cryogel in an aqueous medium, the sponge quickly absorbs the liquid through the system of large, interconnected pores and swells virtually to the original size. This quality of ABCGs is attractive for the seeding of scaffolds with the cells to be cultured (see the Methods section). The inoculation of an insulinoma cell suspension was performed in this manner because capillary forces

sucked in the cells inside the inner space of the spongy ABCG scaffold.

Thermophysical properties of the agarose cryogels

Thermotropic transitions in agarose cryogels were investigated with high-sensitivity differential scanning calorimetry (HS-DSC) and by the measurement of the macroscopic fusion temperature of ABCG specimens (see the Methods section). In the HS-DSC studies, the experimental variables were the temperature of the incubation regimes in a frozen state (−5, −20, and −30°C) and the polysaccharide concentration in the precursor solution (2.5 and 3.0 g/dL). The apparent heat capacity curves of the agarose cryogels are shown in Figure 5(a). All the samples revealed a single heat capacity peak at about 80°C corresponding to the melting of the agarose double helices (helix-to-coil transition). No substantial effect of the cryostructuring conditions on the position and profile of the transition was observed. Values of the thermodynamic parameters (T_t, $\Delta_t h$, and $\Delta_t T$) of the polysaccharide conformational transition in the cryogels are summarized in Table IV. We found that the transition parameters of ABCGs obtained at different frozen storage temperatures and the used concentrations of the precursor solution were similar. The average values of the transition parameters are also given in Table IV, in which one can see that the respective values were alike for ABCGs prepared from the initial 2.5 and 3.0 g/dL agarose solutions.

TABLE IV
Thermophysical Characteristics of the ABCGs

Agarose concentration in the solution before cryostructuring (g/dL)[a]	Temperature of the stage (°C)		Fusion temperature of the ABCG (°C)	HS-DSC data		
	Freezing[b]	Storing frozen[c]		T_t (°C)	$\Delta_t h$ (J/g)	$\Delta_t T$ (°C)
2.5	−30	−5	88.4 ± 0.4	81.3	47	18.5
		−10	88.1 ± 0.7	—	—	—
		−20	87.9 ± 0.6	83.0	40	16.2
		−30	86.7 ± 0.2	83.0	43	16.8
Average				82.4 ± 0.8	43.3 ± 2.4	17.2 ± 0.9
3.0	−30	−5	90.3 ± 0.3	82.1	41	17.1
		−10	89.7 ± 0.5	—	—	—
		−20	88.4 ± 0.4	83.4	40	16.5
		−30	87.3 ± 0.1	83.0	42	17.9
Average				82.8 ± 0.5	41.0 ± 0.7	17.2 ± 0.5

A dash indicates no data.
[a] pH = 12.6.
[b] One hour.
[c] Twenty-three hours.

An important feature of the agarose cryogels is the rather high concentration of polysaccharide in the dispersed phase of the gel (Table III). Note that ordinary agarose hydrogels obtained by the cooling of hot polysaccharide solutions, without experimental hindrances, can usually be prepared at a concentration range of 1–5/6 g/dL. More concentrated aqueous solutions of agarose are extremely viscous and difficult to manipulate, so a more sophisticated technique is required to reproduce the preparation.

It was of interest to compare the thermodynamic properties of the ordinary agarose gels and the cryogels to clarify whether the agarose concentration is important for the gel conformational stability. Figure 5(b) displays the HS-DSC thermograms of ordinary agarose gels of different concentrations. It is evident that a variation in the concentration of the precursor polysaccharide solution does not affect the transition parameters of these gels. The average values of T_t, $\Delta_t h$, and $\Delta_t T$ of the ordinary agarose gels were found to be equal to 84.7 ± 0.6°C, 37 ± 2 J/g, and 19.7 ± 0.6°C, respectively. These values do not differ markedly from the transition parameters of agarose cryogels (Table IV). Consequently, the agarose double helices remained intact in the gels of different concentrations and were not affected by the mode of gel preparation, that is, by the chilling of the initial agarose solution below the gel-set temperature or by the freeze–thaw procedure. Yet, the transparency of the gel matter in the walls (Figs. 1–3), which were virtually uniform in their staining (i.e., the absence of visible, more strongly colored local inclusions), testifies to the homogeneous character of the agarose gel that constitutes the walls.

At the same time, we found certain differences in the values of the fusion temperatures for ABCGs formed under various frozen storage conditions (Table IV). First, cryogels prepared from the 3 g/dL agarose solution fused at temperatures 1–2°C higher in comparison with samples produced with lower polymer concentrations (2.5 g/dL) and cryogenically structured under identical conditions. Because this trend was also inherent in the dry matter content in analogous ABCGs (Table III), one can conclude that registered differences in the ABCG fusion temperatures were due to the differences in the agarose concentration in the gel phase (pore walls) of such spongy cryogels.

Moreover, somewhat more heat resistant were those ABCGs that upon formation were incubated frozen at a warmer subzero temperature. Thus, when fusion temperatures of specimens prepared from the 3 g/dL solution and frozen stored at −5 and −30°C were compared, the former melted at 3°C higher (90.3 vs 87.3°C, respectively). This meant that during the prolonged residence of the frozen system at −5°C, a larger number of fusible intermolecular noncovalent links (mainly cooperative hydrogen bonds) were formed than in the case of frozen storage at −30°C. Note that the gel fusion temperature measured by a falling ball method (see the Methods section) characterizes the macroscopic property of ABCG, that is, its heat resistance as a whole material, and answers to the temperature region in which the most thermally resistant physical junction knots of the 3D network are broken, thus finishing the gel-to-sol transition. Therefore, the values of the gel fusion temperature of ABCGs appreciably exceed the values of the helix-to-coil transition temperature measured with the HS-DSC technique.

Cell morphology and histochemistry of RINm pseudoislets cultured in ABCGs

The ABCGs, prepared and characterized as described in the previous sections, were then used in biological
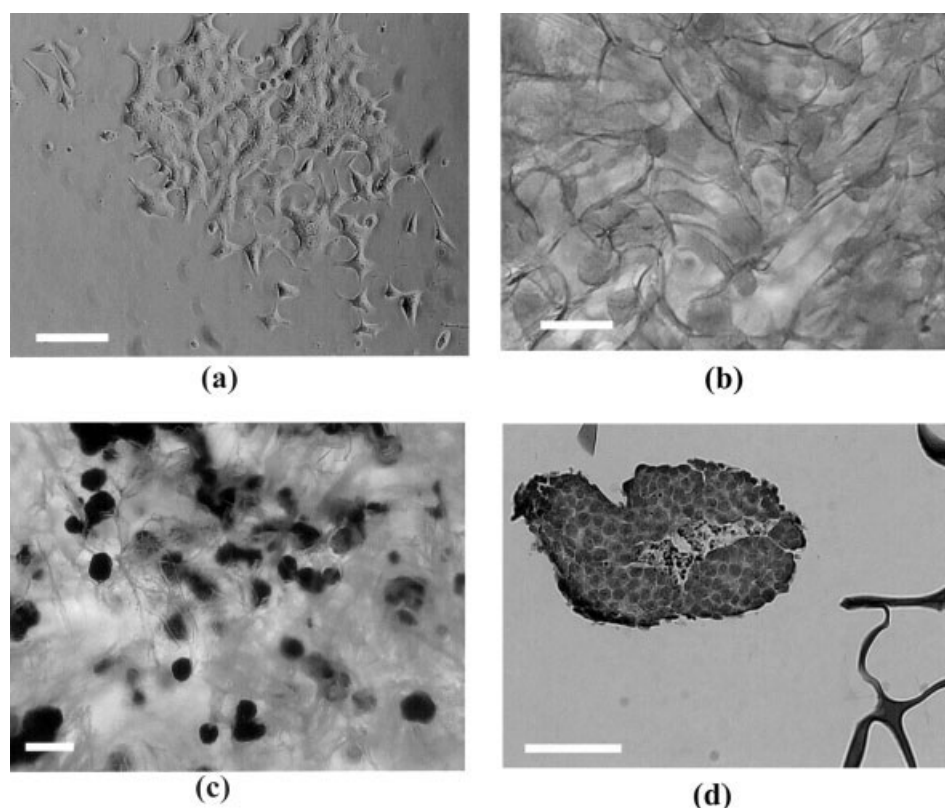
Figure 6 Cell morphology and histochemistry: (a) microphotograph of RINm cells grown as a monolayer cultured on a plastic surface (scale bar = 20 μm), (b) pseudoislets formed in the ABCGs (scale bar = 100 μm), (c) intensive MTT staining of pseudoislets cultured for 10 days in the ABCGs (scale bar = 100 μm), and (d) central necrosis in pseudoislets cultured for 10 days in the ABCGs (H&E staining; scale bar = 100 μm).

experiments as 3D supermacroporous scaffolds for the culturing of insulin-producing cell aggregates. The RINm cells formed a monolayer when cultured on tissue culture plastic [Fig. 6(a)]. However, when the RINm cells were seeded in ABCGs, the cells did not adhere to the agarose surface but, during overnight incubation, formed 3D, multicellular, spherical aggregates [pseudoislets; Fig. 6(b)]. The RINm pseudoislets were about 50–100 μm in diameter, and they did not increase significantly in size during the 10 days in culture. Figure 6(c) shows vital staining of RINm pseudoislets with the MTT reagent, offering evidence of mitochondrial oxidative processes in living cells. However, a histological examination [Fig. 6(d)] revealed signs of necrosis in the core of some pseudoislets following prolonged culture. Similar degenerative changes were also found by other authors for mouse insulinoma cells, line 16 (MIN6) pseudoislets cultured on a gelatin substrate.[46] These degenerative changes probably reflect limitations in the nutrient and oxygen supply to cells located in the central part of pseudoislets cultured *in vitro*. On the other hand, it is known that subcutaneously implanted pseudoislets are able to form an islet-specific microvasculature for nutritional and oxygen supply to cells
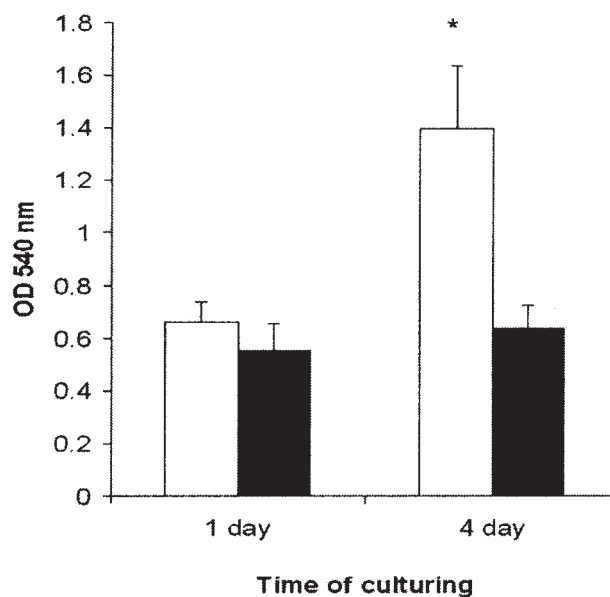

Figure 7 Effect of the ABCGs on cell proliferation, as estimated with the MTT assay. Data are given as means plus or minus standard deviations of three independent experiments. *$P < 0.05$ compared to cells grown as a monolayer for 24 h (white columns represent cells in the monolayer, and black columns represent cells in the cryogel scaffold). OD 540 nm is the optical density at 540 nm.
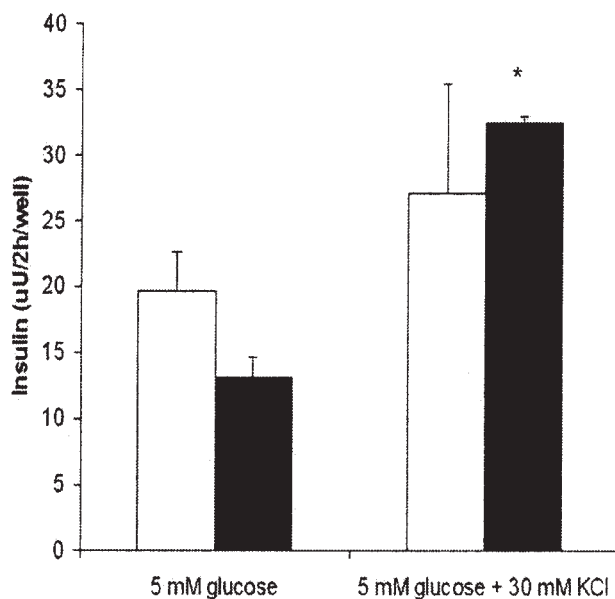
Figure 8 Effect of the cells cultured in the ABCGs on K$^+$-dependent insulin secretion. The cells were incubated in KRBB supplemented with glucose (5 mM) alone and then switched to KRBB supplemented with both glucose (5 mM) and KCl (30 mM). The data are given as means plus or minus standard deviations of three independent experiments. *$P < 0.05$ compared to 5 mM glucose alone (white columns represent cells in the monolayer, and black columns represent cells in the cryogel scaffold).

and adequate blood drainage for insulin liberation, and this suggests that pseudoislets may become a suitable alternative to islet transplantation in diabetes.[30]

Growth and functional activity of RINm pseudoislets cultured in the agarose cryogels

Quantitative measurements of the proliferation of RINm cells cultured in plastic wells and in ABCGs were performed with the MTT assay. Figure 7 shows significant retardation of RINm pseudoislet growth in ABCGs compared to the proliferation of cells attached to the plastic surface. Such growth inhibition is in agreement with our observation of a lack of visible changes in the size of pseudoislets during prolonged culture. This contrasts with the reported observation that cell-to-cell interactions within MIN6 pseudoislets cultured on a gelatin substrate initiate antiproliferative signals but do not reduce cell proliferation after 7 days in culture.[46] Such differences may reflect the importance of the cellular metabolism and scaffold characteristics for the growth behavior of pseudoislets.

To examine the effect of ABCGs on the functional activity of RINm cells, the insulin response to glucose supplemented with 30 mM KCl was evaluated in cells cultivated directly on the plastic surface of culture plates and in RINm pseudoislets cultured in

ABCGs. As shown in Figure 8, pseudoislets in ABCGs demonstrated enhanced K$^+$-dependent insulin secretion in contrast to cells cultured as a monolayer. Interestingly, the stimulation index for insulin release was significantly higher in pseudoislets compared to a cell monolayer (2.48 ± 0.09 vs 1.43 ± 0.64, $P < 0.05$). These results suggest that the formation of RINm pseudoislets in ABCGs improves the functional responsiveness of β-cells. Along with the considerable inner surface area of spongy ABCGs, which can support a large number of cultivated cells, an additional advantage of ABCGs is their sufficient transparency, which allows a microscopic analysis of the cell morphology. Lastly, the macroporosity of the matrix affords improved mass-transfer characteristics within the volume of such 3D scaffolds, which are crucial for cell nutrition and oxygenation.

CONCLUSIONS

Conventional agarose gels are related, as is well known,[13–20] to thermoreversible physical or noncovalent gel systems, and the same is true with respect to agarose cryogels because, for their formation, no chemical crosslinking agents are required. After the preparation of an ABCG, it can be melted by heating above the gel fusion temperature, and the resulting polymer solution can again be transformed into a cryogel via freeze–thaw processing. In this respect, agarose cryogels are akin to other noncovalent cryogels obtained on the basis of diverse macromolecular precursors and studied over approximately the past 25 years (e.g., see refs. 1, 34, and 35). Some of these cryogels are macroporous matrices (with a pore size of a micrometer level), such as those produced from highly saponificated PVA,[34,35,47] amylopectin,[48,49] and some polygalactomannans;[50–52] other cryogels possess a supermacroporous, spongelike morphology (with a pore size ranging from tens to hundreds of micrometers), such as cryogels fabricated from solutions of gelatin,[47] starch,[53] and β-glucan.[54,55] Their physicochemical properties depend on many factors but particularly on the characteristics of the proper gel precursor, its initial concentration, and the conditions of cryotropic gel formation. In this study, we showed how some of these factors can influence the properties and morphology of ABCGs. In addition, the data of our previous work,[7] as well as the results of ABCG biotesting carried out in this study, offer the promise of potential applications of these supermacroporous matrices as biocompatible 3D scaffolds for cell culture.

References

1. Lozinsky, V. I. Russ Chem Rev 2002, 71, 489.
2. Lozinsky, V. I.; Galaev, I. Y.; Plieva, F.; Mattiasson, B. Bioseparation 2001, 10, 163.
3. Lozinsky, V. I.; Galaev, I. Y.; Plieva, F.; Savina, I. N.; Jungvid, H.; Mattiasson, B. Trends Biotechnol 2003, 21, 445.
4. Arvidsson, P.; Plieva, F. M.; Savina, I. N.; Lozinsky, V. I.; Fexby, S.; Bulow, L.; Galaev, I. Y.; Mattiasson, B. J Chromatogr A 2002, 977, 27.
5. Kumar, A.; Plieva, F. M.; Galaev, I. Y.; Mattiasson, B. J Immunol Methods 2003, 283, 185.
6. Williams, S. L.; Eccleston, M. E.; Slater, N. K. H. Biotechnol Bioeng 2005, 89, 783.
7. Bloch, K.; Lozinsky, V. I.; Galaev, I. Y.; Yavriyanz, K.; Vorobeychik, M.; Azarov, D.; Damshkaln, L. G.; Mattiasson, B.; Vardi, P. J Biomed Mater Res A 2005, 75, 802.
8. Kumar, A.; Bansal, V.; Andersson, J.; Roychoudhury, P. K.; Mattiasson, B. J Chromatogr A 2006, 1103, 35.
9. Araki, C. H. Bull Chem Soc Jpn 1956, 29, 43.
10. Araki, C.; Arai, K. Bull Chem Soc Jpn 1967, 40, 1452.
11. Lahaye, M.; Rochas, C. Hydrobiologia 1991, 126, 137.
12. Armisén, R.; Galatas, F. In Handbook of Hydrocolloids; Phillips, G. O.; Williams, P. A., Eds.; Woodhead: London, 2000; p 21.
13. Letherby, M. R.; Young, D. A. J Chem Soc Faraday Trans I 1981, 77, 1953.
14. Tako, M.; Nakamura, S. Carbohydr Res 1988, 180, 277.
15. Nishinari, K. Colloid Polym Sci 1997, 275, 1093.
16. Hayashi, A.; Kinoshita, K.; Yasueda, S. Polym J 1980, 12, 447.
17. Burchard, W. Brit Polym J 1985, 17, 154.
18. Watase, M.; Nishinari, K.; Clark, A. H.; Ross-Murphy, S. B. Macromolecules 1989, 22, 1196.
19. Braudo, E. E.; Muratalieva, I. R.; Plaschina, I. G.; Tolstoguzov, V. B.; Markovich, I. S. Colloid Polym Sci 1991, 269, 1148.
20. Aymard, P.; Martin, D. R.; Plucknett, K.; Foster, T. J.; Clark, A. H.; Norton, I. T. Biopolymers 2001, 59, 131.
21. Gruber, H. E.; Fisher, E. C.; Desai, B.; Stasky, A. A.; Hoelscher, G.; Hanley, E. N. Exp Cell Res 1997, 235, 13.
22. Wang, W.; Gu, Y.; Tabata, Y.; Miyamoto, M.; Hori, H.; Nagata, N.; Touma, M.; Balamurugan, A. N.; Kawakami, Y.; Nozawa, M.; Inoue, K. Transplantation 2002, 73, 122.
23. Stokols, S.; Tuszynski, M. H. Biomaterials 2004, 25, 5839.
24. Gruber, H. E.; Hoelscher, G. L.; Leslie, K.; Ingram, J. A.; Hanley, E. N. Biomaterials 2006, 27, 371.
25. Stokols, S.; Tuszynski, M. H. Biomaterials 2006, 27, 443.
26. Raghunath, J.; Rollo, J.; Sales, K. M.; Butler, P. E.; Seifalian, A. M. Biotechnol Appl Biochem 2007, 46, 73.
27. Malafaya, P. B.; Silva, G. A.; Reis, R. L. Adv Drug Delivery Rev 2007, 59, 207.
28. Luther, M. J.; Hauge-Evans, A.; Souza, K. L. A.; Jorns, A.; Lenzen, S.; Persaud, S. J.; Jones, P. M. Biochem Biophys Res Commun 2006, 343, 99.
29. Hauge-Evans, A. C.; Squires, P. E.; Persaud, S. J.; Jones, P. M. Diabetes 1999, 48, 1402.
30. Beger, C.; Cirulli, V.; Vajkoczy, P.; Halban, P. A.; Menger, M. D. Diabetes 1998, 47, 559.
31. Lozinsky, V. I.; Damshkaln, L. G.; Plieva, F. M.; Galaev, I. Y.; Mattiasson, B. Rus. Pat. 2220987 (2001).
32. Mikheeva, L. M.; Grinberg, N. V.; Mashkevich, A. Y.; Grinberg, V. Y.; Thanh, L. T. M.; Makhaeva, E. E.; Khokhlov, A. R. Macromolecules 1997, 30, 2693.
33. Bloch, K.; Vorobeychyk, M.; Yavriyants, K.; Vardi, P. Biochem Pharmacol 2003, 65, 1797.
34. Lozinsky, V. I. Russ Chem Rev 1998, 67, 573.
35. Hassan, C. M.; Peppas, N. A. Adv Polym Sci 2000, 153, 37.
36. Labudzinska, A.; Ziabicki, A. Kolloid Z Z Polym 1971, 243, 21.
37. Yakoyama, F.; Achife, E. C.; Momoda, J.; Shimamura, K.; Monobe, K. Colloid Polym Sci 1990, 268, 552.
38. Lozinsky, V. I.; Morozova, S. A.; Vainerman, E. S.; Titova, E. F.; Shtil'man, M. I.; Belavtseva, E. M.; Rogozhin, S. V. Acta Polym 1989, 40, 8.
39. Sergeev, G. B.; Batyuk, V. A. Russ Chem Rev 1976, 45, 391.
40. Van Vlierberghe, S.; Cnudde, V.; Dubruel, P.; Cosijns, A.; De Paepe, I.; Jacobs, P. J. S.; Van Hoorebeke, L.; Remon, J. P.; Schacht, E. Biomacromolecules 2007, 8, 331.
41. Lozinsky, V. I.; Vainerman, E. S.; Titova, E. F.; Belavtseva, E. M.; Rogozhin, S. V. Colloid Polym Sci 1984, 262, 769.
42. Lozinsky, V. I.; Vainerman, E. S.; Korotaeva, G. F.; Rogozhin, S. V. Colloid Polym Sci 1984, 262, 617.
43. Larsson, P.-O. (Sweden) Pat. WO 93/19115 (1993).
44. Gustavsson, P.-E.; Larsson, P.-O. J Chromatogr A 1996, 734, 231.
45. Gustavsson, P.-E.; Larsson, P.-O. J Chromatogr A 1999, 832, 29.
46. Luther, M. J.; Davies, E.; Muller, D.; Harrison, M.; Bone, A. J.; Persaud, S. J.; Jones, P. M. Am J Physiol Endocrinol Metab 2005, 288, E502.
47. Rogozhin, S. V.; Lozinsky, V. I.; Vainerman, E. S.; Domotenko, L. V.; Mamtsis, A. M.; Ivanova, S. A.; Shtil'man, M. I.; Korshak, V. V. Dokl Akad Nauk 1984, 278, 129 (in Russian).
48. Lozinsky, V. I.; Damshkaln, L. G.; Brown, C. R. T.; Norton, I. T. J Appl Polym Sci 2000, 75, 1740.
49. Lozinsky, V. I.; Damshkaln, L. G.; Brown, C. R. T.; Norton, I. T. J Appl Polym Sci 2000, 78, 371.
50. Tanaka, R.; Hatakeyama, T.; Hatakeyama, H. Polym Int 1998, 45, 118.
51. Lozinsky, V. I.; Damshkaln, L. G.; Brown, C. R. T.; Norton, I. T. Polym Int 2000, 49, 1434.
52. Doyle, J. P.; Giannouli, P.; Martin, E. J.; Brooks, M.; Morris, E. R. Carbohydr Polym 2006, 64, 391.
53. Schulze, W. E.; Yu, D. T.; MacMasters, M. M. Stärke 1964, 16, 41.
54. Lazaridou, A.; Biliaderis, C. G. Food Hydrocolloids 2004, 18, 933.
55. Vaikousi, H.; Biliaderis, C. G. Food Chem 2005, 91, 505.